

Identification of Potential Novel Pleiotropic Susceptibility Variants Common To Lumbar Spine Bone Mineral Density And Birth Weight

Yu-Qian Song (✉ 1553661809@qq.com)

The Third Affiliated Hospital of Southern Medical University <https://orcid.org/0000-0002-3152-4398>

Shi-Di Hu

The Third Affiliated Hospital of Southern Medical University

Xu Lin

First Peoples Hospital of Shunde: Shunde Hospital of Southern Medical University

Xiang-He Meng

Central South University

Xiao Wang

First Peoples Hospital of Shunde: Shunde Hospital of Southern Medical University

Yin-Hua Zhang

The Third Affiliated Hospital of Southern Medical University

Cheng Peng

Guangzhou First People's Hospital

Rui Gong

Gansu Provincial Hospital

Tao Xu

University of Iowa Health Science Library: The University of Iowa

Tong Zhang

The Third Affiliated Hospital of Southern Medical University

Chen-Zhong Li

The Third Affiliated Hospital of Southern Medical University

Dao-Yan Pan

The Third Affiliated Hospital of Southern Medical University

Jia-Yi Yang

The Third Affiliated Hospital of Southern Medical University

Jonathan Greenbaum

Tulane University

Jie Shen

First Peoples Hospital of Shunde: Shunde Hospital of Southern Medical University

Hong-Wen Deng

Research Article

Keywords: Osteoporosis, Bone Mineral Density, Birth Weight, Pleiotropy, Conditional False Discovery Rate

Posted Date: June 30th, 2021

DOI: <https://doi.org/10.21203/rs.3.rs-633182/v1>

License:   This work is licensed under a Creative Commons Attribution 4.0 International License.

[Read Full License](#)

Abstract

An increasing number of epidemiological studies have suggested that birth weight (BW) may be a determinant of bone health later in life, although the underlying genetic mechanism remains unclear. Here, we applied a pleiotropic conditional false discovery rate (cFDR) approach to the genome-wide association study (GWAS) summary statistics for lumbar spine bone mineral density (LS BMD) and BW, aiming to identify novel susceptibility variants shared between these two traits. We detected 5 novel potential pleiotropic loci which are located at or near 7 different genes (*NTAN1*, *PDXDC1*, *CACNA1G*, *JAG1*, *FAT1P1*, *CCDC170*, *ESR1*), among which *PDXDC1* and *FAT1P1* have not previously been linked to these phenotypes. To partially validate the findings, we demonstrated that the expression of *PDXDC1* was dramatically reduced in ovariectomized (OVX) mice in comparison with sham-operated (SHAM) mice in both the growth plate and trabecula bone. Furthermore, immunohistochemistry assay with serial sections showed that both osteoclasts and osteoblasts express *PDXDC1*, supporting its potential role in bone metabolism. In conclusion, our study provides insights into some shared genetic mechanisms for BMD and BW as well as a novel potential therapeutic target for the prevention of OP in the early stages of the disease development.

Key Messages

- We investigated pleiotropy-informed enrichment between LS BMD and BW.
- We identified genetic variants related to both LS BMD and BW by utilizing a cFDR approach.
- *PDXDC1* is a novel pleiotropic gene which may be related to both LS BMD and BW.
- Elevated expression of *PDXDC1* is related to higher BMD and lower ratio n-6/n-3 PUFA indicating a bone protective effect of *PDXDC1*.

Introduction

It was recently reported that more than 200 million Chinese would suffer from Osteoporosis (OP) or low bone mass [1], and that the prevalence in the US was projected to increase by 17.2 million between 2010 and 2030 [2]. The lifetime fracture risk of patients with OP is estimated to be as high as 40% [3], and the economic burden associated with fractures is predicted to exceed \$25 billion by 2050 without effective intervention of OP risk [4].

In recent decades, growing epidemiological evidence has shown that birth weight (BW) may be an important determinant of adult bone health. For instance, a previous study in British twins (n = 4008, 100% women) found that elevated BW has a protective effect on both bone mass and bone mineral content [5]. Similarly, research from The Gambia (n = 120, 57% men and 43% women) indicated that BW is positively correlated with the cross sectional bone area at cortical sites in men and at trabecular sites in women [6]. Additionally, several studies have suggested that the intrauterine environment may program the embryogenesis genome with a skeletal growth trajectory that persists post-partum independent of post-natal factors [7, 8]. Given the close relationship between BW and bone health, and the high

heritability of BW (87%)[9] and bone mineral density (BMD) (75%-83%)[10], we hypothesize there may be shared genetic determinants contributing to these two phenotypes.

Previous genome-wide association studies (GWAS) have identified at least 90 lumbar spine (LS) BMD-related loci and 87 BW-related loci, yet collectively these can only explain 12% and 15% of the individual trait variations, respectively [11, 12]. Here, we jointly analyzed GWAS summary statistics for BW and LS BMD using a pleiotropic conditional false discovery rate (cFDR) approach to identify novel trait-associated loci for the individual traits as well as those that may overlap [13]. The cFDR technique augments the effective sample size by efficiently combining existing datasets and has been successfully utilized by our team and others for exploring common pleiotropic loci for two related complex traits, such as coronary artery disease (CAD) and BMD [10], CAD and body mass index [14] or height and BMD [15].

The aim of this study was to identify potential novel pleiotropic susceptibility variants common to both BW and LS BMD using the cFDR method. Furthermore, to partially validate the reliability of the method and the genes identified by cFDR, we selected a novel pleiotropic gene to perform functional validation experiments in mice.

Materials And Methods

GWAS data sets

BMD measured by dual-energy X-ray absorptiometry (DXA) is the gold standard for OP diagnosis as recommended by the WHO. Since LS BMD is estimated to have the highest heritability among commonly measured skeletal sites [16] it was thus chosen for studying the relationship between BMD and BW in this genetic association analysis.

The LS BMD GWAS summary-statistic dataset was acquired from the Genetic Factors for Osteoporosis Consortium (GEFOS), and included of 53,236 individuals of European ancestry [17]. At the present time, it is the largest GWAS for DXA derived BMD measurements. The BW summary statistics were downloaded from the Early Growth Genetics (EGG) Consortium, and included 143,677 subjects of European ancestry [12]. To confirm that the variance estimated for each single-nucleotide polymorphism (SNP) was not inflated due to population stratification, standard genomic control procedures were applied to the two original GWAS studies.

SNP pruning and merging

We performed linkage disequilibrium (LD)-based pruning for each dataset using PLINK version 1.9 software. Firstly, the LD was computed for each pair of SNPs in a window containing 50 SNPs. For pairs with an $r^2 > 0.2$, the SNP with the smaller minor allele frequency was removed. The window was moved 5 SNPs forward, and the procedure was repeated until no pairs of SNPs across the genome had $r^2 > 0.2$. The pruning was based on the LD structure of the CEU HapMap 3 genotypes. After the pruning process was completed, there were 121,848 SNPs which overlapped between BMD and BW which were retained for the subsequent analysis.

Estimation of pleiotropic enrichment

Stratified Quantile-quantile plots (Q-Q plots) were constructed to visualize the pleiotropic enrichment between LS BMD and BW when conditioning on successively more stringent p -value thresholds of the conditional trait: $p < 1$ (all SNPs), $p < 0.1$, $p < 0.01$ and $p < 0.001$. The observed p -values of the principal trait, denoted as “nominal $-\log_{10}(p)$ ”, were plotted against the cumulative distribution function of observed p -values, denoted as “empirical $-\log_{10}(q)$ ”. The line $x = y$ indicates the null hypothesis of no pleiotropic enrichment, and plots that deviate leftward from the null line indicate that a pleiotropic effect exists between the traits[13].

Calculation of cFDR and conjunction cFDR (ccFDR)

The calculation of the cFDR extends from the single phenotype case, where the unconditional false discovery rate (FDR) for a set of SNPs is characterized as the probability of a false positive association. The cFDR expands this idea to the two-phenotype case and is defined as the probability of a false positive association with the principal trait given that the association p -values with both the principal and conditional traits are at least as small as the observed p -values. Using the GWAS summary statistics, the cFDR for each SNP was separately computed for both orderings of the traits (BMD|BW and BW|BMD, where “|” indicates conditional upon). The SNPs were regarded as significantly related to the principal trait when $\text{cFDR} < 0.05$. The ccFDR value was defined as the maximum cFDR value of two trait orderings, and SNPs with $\text{ccFDR} < 0.05$ were interpreted as pleiotropic loci associated with both traits. As the cFDR method has been widely published and successfully utilized both by our team [10] and other teams [14, 15], the specific procedure and formulae for calculation will not be detailed in this article. Manhattan plots were constructed using R to graphically display the genomic locations of significant variants.

Annotation of novel SNPs and genes

The significant cFDR SNPs ($\text{cFDR} < 0.05$) were queried using the SNPinfo web server (<https://snpinfo.niehs.nih.gov>) to ascertain all corresponding SNPs with high LD ($r^2 > 0.8$). All SNPs (including those with $\text{cFDR} < 0.05$ and those with high LD) were then compared to previous GWAS findings ($p\text{-value} < 5 \times 10^{-8}$) on the European Bioinformatics Institute website. SNPs with a GWAS p -value $> 5 \times 10^{-8}$ that have not been reported as having an association with BMD or/and BW were considered to be potential novel SNPs. We utilized both the SNP and CNV Annotation Database (SCAN, <http://scandb.org/newinterface/about.html>) and PubMed (<https://www.ncbi.nlm.nih.gov/gene>) to map the significant cFDR SNPs to nearby genes. Genes that were not previously identified in BMD or/and BW-related studies were deemed novel.

Functional enrichment analysis and protein–protein interaction analysis of identified genes

To establish the physiological role of genes of interest, we performed functional enrichment analysis using the Database for Annotation, Visualization and Integrated Discovery (DAVID, <https://david.ncifcrf.gov/summary.jsp>). To explore the functional interactions between proteins produced

by cFDR-significant pleiotropic susceptibility genes, we performed protein–protein interaction analysis by the online tool STRING 10.0 (<http://string-db.org/>).

Fine-mapping

To discover putative pleiotropic causal SNPs and prioritize genes for the subsequent functional experiments, we performed multi-trait fine mapping analysis using PAINTOR[18]. In particular, we focused on a potential OP susceptibility locus located on chromosome 16 (14800000-16280000) which includes the gene *PDXDC1*.

Postmenopausal OP mouse models

Female C57BL/6 mice were obtained from the Animal Center of Southern Medical University, which either received sham-operated (SHAM) surgery or ovariectomy (OVX) under 1.2% tribromoethanol anesthesia at 8 weeks of age. The OVX group had bilateral ovary removal, while the SHAM group had a similar volume of adipose tissue removed from around the ovaries. The mice were sacrificed sixteen weeks post-surgery and hind-limb specimens were harvested for subsequent analyses. Four mice were randomly selected from each experimental group.

Micro-computed tomography analysis

The hindlimbs were fixed in 4% paraformaldehyde for 48 h then scanned in a micro-computed tomography (micro-CT) scanner (Viva CT40, Scanco Medical AG, Bassersdorf, Switzerland). Morphological analysis was conducted on trabecular bone. The region of interest in the trabecular bone began at a position 20 spongiosa slices (9 µm thick) from the lower growth plate of the femur and finished 160 slices later. Bone volume/total volume (BV/TV), trabecular thickness (Tb. Th), trabecular number (Tb. N), and trabecular separation (Tb. Sp) were computed using standard three-dimensional microstructural analysis.

Immunohistochemistry

The hindlimbs were fixed in 4% paraformaldehyde in phosphate-buffered saline (PBS) for 48 h at 4°C, then decalcified in 10% ethylenediaminetetraacetic acid (EDTA; pH 7.4) for 21 days at room temperature prior to dehydration in a rising gradient of ethanol and embedded in paraffin. The tissues were sliced into 3 or 4 micron thick sections for histological analysis. Tissue sections were incubated overnight at 4°C with *PDXDC1* primary antibody (Proteintech, 21021-1-AP, 1:200) then for 1 h at room temperature with a secondary antibody (Arigo, ARG65351, 1:200). Diaminobenzidine (DAB, KGP1045/KGP1045-20/KGP1045-100, 1:1:1:20) was conjugated to the secondary antibody.

Both *PDXDC1*-positive and the total number of cells were enumerated (at 400× magnification) at the growth plate and within the trabecula bone in the femur or tibia. Four views from these regions picked at random were counted on each section, and three consecutive sections were selected for each mouse.

To distinguish whether the *PDXDC1*-positive cells were osteoclasts or osteoblasts, we conducted immunohistochemistry assay with three-micrometer-thick serial sections in the SHAM group. Tartrate-resistant acid phosphatase (TRAP) is a specific marker of osteoclasts and osteocalcin (OCN) is a specific marker of osteoblasts. The specific procedures of the immunohistochemistry assay with serial sections were as follows: 1) there were two thin and consecutive tissue sections on each glass slide labeled A and B in advance, 2) A-labeled sections were incubated with *PDXDC1* primary antibody (Proteintech, 21021-1-AP, 1:200). B-labeled sections were incubated with anti-OCN primary antibody (abcam, ab93876, 1:500) or subjected to TRAP staining (Sigma-Aldrich), 3) sections not used for TRAP staining were incubated with suitable secondary antibody (Arigo, ARG65351, 1:200).

***fat-1* transgenic (TG) mouse model**

To preliminarily verify the mechanism of *PDXDC1* affecting BW and BMD, a *fat-1* TG mouse model was adopted. Male *fat-1* TG mice were matched with wild-type (WT) female C57BL/6 mice to breed *fat-1* gene-positive mice. The *fat-1* gene-positive mice were identified using genomic DNA extracted from tail biopsies. Primer sequences were as follows: 5'-GGACCTGGTGAAGAGCATCCG-3' and reverse, 5'-GCCGTGCAGAAAGCCAAAC-3'. We fed the mice until 16 months old when they were sacrificed and hind-limb specimens were harvested for subsequent analysis. We performed the immunohistochemical assay on both *fat-1* TG mice and WT mice with *PDXDC1* primary antibody (Proteintech, 21021-1-AP, 1:200).

Sections were imaged using a Zeiss microscope (Carl Zeiss, New York, USA). All experiments were performed three times or more for reproducibility.

Statistics

Data shown are means \pm standard deviation (SD). Two sample t-tests were performed for comparison of experimental groups. Statistical significance was set at p -value < 0.05 .

Mendelian randomization (MR) analysis

To investigate the potential causal relationship between BW and LS BMD, we performed two-sample MR analysis using the BW-associated SNPs as instrumental variables. [19]. The causal effects from multiple instruments were combined using several meta-analysis approaches including maximum likelihood estimation and inverse-variance weighting (IVW).

Results

Pleiotropy between LS BMD and BW

The conditional Q-Q plots for LS BMD at various nominal p -values of association with BW demonstrate enrichment over the null hypothesis line (i.e. leftward shift) at each stratified level of significance for BW (Fig. 1a), and vice versa for BW SNPs conditioned on LS BMD (Fig. 1b).

LS BMD variants identified by cFDR

22 LS BMD-associated SNPs conditioned on BW, mapping to 10 different chromosomes, were identified using the cFDR method (Fig. 2a). Among these 22 SNPs, 10 had a p -value less than 5×10^{-8} in the original LS BMD GWAS [17], and 1 SNP (*rs2741856*) was previously associated with BMD in another GWAS [20]. These 11 SNPs had therefore successfully replicated previous GWAS, partially demonstrating the reliability and robustness of the cFDR method. The remaining 11 novel SNPs with a p -value $> 5 \times 10^{-8}$, would have easily been overlooked in a traditional single trait GWAS. The 22 SNPs were physically mapped to 27 different genes (**Online Resource 1**), 15 of which had previously been reported to be related to BMD or OP in various other studies[20–26]. In functional term enrichment analysis, some the identified variants were enriched in several terms associated with bone metabolism, such as “regulation of bone remodeling”, “regulation of bone resorption” and “skeletal system development” (Table 1).

Table 1
Functional term enrichment analysis

GO Term	count	p value	FDR
LS BMD genes			
regulation of bone remodeling	2	1.2E-2	8.1E-1
regulation of bone resorption	2	1.2E-2	8.1E-1
skeletal system development	3	2.6E-2	8.4E-1
BW genes			
insulin-like growth factor receptor signaling pathway	5	5.1E-7	4.9E-4
insulin receptor binding	5	1.4E-5	1.9E-3
phosphatidylinositol 3-kinase signaling	4	3.0E-4	9.2E-2
positive regulation of MAPK cascade	5	6.6E-4	1.0E-1
protein binding	55	5.3E-3	1.9E-1
regulation of growth	6	3.9E-2	4.2E-1
Column definition: GO Term, gene ontology term.			

BW variants identified by cFDR

Conditioned on the association with LS BMD, 99 BW-associated SNPs mapping to 20 different chromosomes (Fig. 2b), were identified as being associated with BW using the cFDR method. Among the 99 SNPs, 16 had a p -value less than 5×10^{-8} in the original GWAS [12]. The remaining 83 SNPs with p -values $> 5 \times 10^{-8}$, easily overlooked in traditional studies, were considered to be novel SNPs. The 99 SNPs were mapped to 130 different genes (**Online Resource 2**). Among these 130 different genes, 31 had been identified as having an association with BW in previous studies[10, 12, 27–33]. The functional term

enrichment analysis results demonstrate that a considerable number of variants were enriched in terms such as “insulin-like growth factor receptor signaling pathway”, “insulin receptor binding”, “phosphatidylinositol 3-kinase signaling”, “positive regulation of MAPK cascade”, “protein binding”, “regulation of growth” (Table 1). Notably, the abnormal expression and/or activation of IGF-1 receptor, phosphatidylinositol 3-kinase signal pathway and MAPK family were confirmed to be associated with intrauterine growth restriction of placentas [34]. Furthermore, vitamin D-binding protein, adipocyte fatty acid-binding protein and insulin-like growth factors binding proteins, have been reported to have a key role in modulating BW [35–37].

Pleiotropic variants for both LS BMD and BW identified by ccFDR

We identified 5 pleiotropic susceptibility SNPs (ccFDR < 0.05) associated with both LS BMD and BW (*rs34955778*, *rs198542*, *rs2423512*, *rs12197879*, *rs1293935*), which mapped to 4 different chromosomes and 7 different genes (Fig. 2c, Table 2). Among these genes, *CACNA1G*, *JAG1*, and *ESR1* were previously reported to be related to both BMD [21, 24] and BW [10, 12], while *CCDC170* and *NTAN1* were previously reported to have an association with BMD [21, 25]. The remaining 2 genes (*PDXDC1* and *FAT1P1*) have not previously been identified to be associated with either trait.

Table 2
Pleiotropic SNPs for both LS BMD and BW

	SNP	Nearby Gene	CHR	cFDR.LS	cFDR.BW	ccFDR
1	rs12197879	CCDC170	6	1.01E-06	2.55E-02	2.55E-02
2	rs1293935	CCDC170 ESR1	6	3.95E-06	2.80E-09	3.95E-06
3	rs34955778	NTAN1 PDXDC1	16	3.59E-02	1.60E-02	3.59E-02
4	rs198542	CACNA1G	17	1.49E-02	1.74E-02	1.74E-02
5	rs2423512	JAG1 FAT1P1	20	8.36E-03	9.41E-06	8.36E-03
Column definition: SNP, single nucleotide polymorphisms; CHR, chromosome; cFDR.LS, conditional false discovery rate of LS BMD when conditioned on BW; cFDR.BW, conditional false discovery rate of BW when conditioned on LS BMD; ccFDR, conjunction conditional false discovery rate.						

PDXDC1 was connected with *CCDC170* and *NTAN1* in the protein-protein interaction network constructed for the cFDR-significant pleiotropic susceptibility genes (Fig. 3), hinting at a potential role for *PDXDC1* in bone health [21].

Fine-mapping

Based on the multi-trait fine mapping analysis, the SNP *rs1121*, which is located in the intron region of *PDXDC1*, was identified to have the highest posterior probability of causality (0.99) for both traits (**Fig. 4**). Additionally, this putative pleiotropic causal SNP is an expression quantitative trait loci (eQTL) associated with *PDXDC1* expression in muscle skeletal tissue (p -value = 9.58×10^7) in the GTEx database (<https://www.gtexportal.org/home/index.html>). Furthermore, *PDXDC1* has been linked with both omega-3 (n-3) and omega-6 (n-6) polyunsaturated fatty acids (PUFAs) in previous GWAS [38, 39]. We note that n-3 and n-6 PUFAs were demonstrated to be critical for both fetal growth and the regulation of bone metabolism [40, 41]. It was reported that elevated n-6/n-3 PUFA ratio is related to lower BMD of hip [42]. Based on these findings, we hypothesized that *PDXDC1* might causally influence BW and BMD through the modulation of PUFAs levels.

Partial validation based on animal models

PDXDC1 was selected as the target gene to test for its association with LS BMD by immunohistochemical analysis for its protein levels in a postmenopausal OP mouse model to partially verify the validity of the cFDR method. Sixteen weeks after ovariectomy, morphometry analysis of trabecular bone demonstrated significantly lower BV/TV (p -value < 0.05), less Tb. N (p -value < 0.01) and wider Tb. Sp (p -value < 0.01) in the OVX group compared to the SHAM group. Tb. Th between the two groups was not significantly different (**Fig. 5a, b**). The immunohistochemical assay showed that quantities of *PDXDC1*-positive cells were present within the growth plate and on the surface of trabecula bone. The expression of *PDXDC1* in the growth plate and trabecula bone of the OVX group decreased dramatically compared to the SHAM group (p -value < 0.0001) (**Fig. 5c**). The immunohistochemistry assay with serial sections showed that both osteoclasts and osteoblasts expressed *PDXDC1* (**Fig. 5d, e**).

To preliminarily verify the mechanism of *PDXDC1* affecting BW and BMD, we performed the immunohistochemical assay on *fat-1* TG mice and WT mice. The *fat-1* TG mice can convert n-6 to n-3 PUFAs endogenously, and have been shown to display elevated n-3 PUFAs and lower n-6 PUFAs in both cartilage and serum [43]. We performed PCR genotyping identification with *fat-1* fragment-specific primers to identify the *fat-1* TG mice (**Fig. 6**). The immunohistochemical assay results showed that the expression of *PDXDC1* in the growth plate of *fat-1* TG mice was increased dramatically compared to WT mice (**Fig. 5f**). This suggests that *PDXDC1* may have a protective role for BMD by interacting with n-3 and n-6 PUFAs.

Two-sample MR analysis

We obtained 46 independent SNPs that associated with BW which were included in the MR analysis. However, we were not able to detect a significant causal effect of BW on BMD (**Online Resource 3**).

Discussion

In this study, we investigated pleiotropy-informed enrichment between LS BMD and BW and identified genetic variants related to both traits by utilizing a cFDR approach. With a cFDR-significance threshold of

0.05, we identified 22 SNPs associated with LS BMD, including 11 novel loci overlooked in previous GWAS [17, 20], 99 SNPs associated with BW, including 83 novel loci ignored in the original GWAS [12], and 5 novel pleiotropic loci which may be related to both LS BMD and BW.

Interestingly, since the variants identified as being associated with either LS BMD or BW by cFDR were conditioned on one another, several may demonstrate pleiotropic effects. For example, *HMGA2*, identified to be associated with BW in this study in addition to other research [44], has also been reported to influence trabecular BMD in elderly men [45]. Additionally, the expression of *HMGA2* has been detected in the human fetal osteoblast cell line hFOB [45]. *WNT4*, identified as being associated with LS BMD by cFDR, was previously reported to be associated with BW in a large scale GWAS [12]. *IGF-1*, identified to be associated with BW by cFDR, was established to regulate BMD in women in a population-based study [46]. It has been proposed that that *IGF-1* may be modulated by changes in estrogen levels, which in turn affects BMD [46]. Lastly, *RB1*, identified to be associated with BW in this study, has been confirmed to be related to mineralization defects in bones in a previous animal study [47].

The 5 identified pleiotropic susceptibility loci for both LS BMD and BW were mapped to 7 different genes, among which *PDXDC1* and *FAT1P1* not previously been linked to these phenotypes are particularly interesting. *PDXDC1*, preferentially expressed in the intestine, encodes the protein vitamin B6-dependent decarboxylase [48]. This gene has been reported to have an association with both n-3 and n-6 PUFAs [38, 39]. We demonstrated that the expression of *PDXDC1* in OVX mice was significantly reduced compared to SHAM group mice. Additionally, the expression of *PDXDC1* in *fat-1* TG mice increased dramatically compared to WT mice. The findings indicate that elevated expression of *PDXDC1* is related to higher BMD and lower ratio n-6/n-3 PUFA. We also successfully verified that both osteoclasts and osteoblasts express *PDXDC1*. These results are in accordance with previous studies in both humans and mice which reported that lower n-6/n-3 PUFA ratio is beneficial for bone health [42, 49]. Both n-3 and n-6 PUFAs have been shown to modulate the function of osteoclasts and osteoblasts through cell adhesion [41]. Furthermore, n-3 PUFAs of maternal blood were found to be positively correlated with BW by reducing blood viscosity and increasing placental blood flow [50]. In future follow-up studies, we may develop *PDXDC1* knockout mice to explore the molecular mechanisms of how *PDXDC1* interacting with n-3 and n-6 PUFAs regulate BW and BMD concurrently. *FAT1P1* is a pseudogene of *FAT1*, and we know limitedly.

Although we successfully applied the cFDR methodology to identify novel variants associated with BW and/or BMD, there are several limitations to the current research. Firstly, we cannot assess the proportion of variability in the phenotypic traits explained by the identified loci since we could not obtain the individual level genotype data. Secondly, we were not able to distinguish between the pleiotropic scenarios where either the variant separately influences both traits or the variant influences BW which in turn influences BMD. Thirdly, our research did not verify the molecular mechanisms of *PDXDC1* concurrently regulating BW and BMD. However, theoretical and biological investigation may be pursued in future studies to reveal the common pathophysiological mechanisms of both traits.

In conclusion, our study indicates that *PDXDC1* may benefit to bone health and provides insights into some shared genetic mechanisms for BMD and BW as well as a novel potential therapeutic target for the prevention of OP in the early stages of the disease development.

Declarations

Availability of data and material The authors confirm that the data and material supporting the findings of this study are available within the article and its supplementary materials.

Consent for publication Not applicable.

Consent to participate Not applicable.

Code availability Not applicable.

Ethics approval All the experimental protocols were approved by the Southern Medical University Animal Care and Use Committee.

Acknowledgements Hong-Wen Deng was partially supported by grants from the National Institutes of Health [R01AR057049, R01AR059781, R01MH107354, R01MH104680, R01GM109068, U19AG055373, R01AR069055] and the Edward G. Schlieder Endowment fund to Tulane University. Jie Shen was partially supported by grants from the Science and Technology Program of Guangzhou, China [201604020007], and the National Natural Science Foundation of China [81770878]. Shi-Di Hu was partially supported by the National Natural Science Foundation of China [81800794] and the PhD Start-up Fund of Natural Science Foundation of Guangdong Province, China [2017A030310390]. Cheng Peng was supported by Medical Science and Technology Foundation of Guangdong Province, Guangdong, China [A2019005] and Guangzhou Planed Project of Science and Technology, Guangzhou, China [201903010091]. We acknowledge the GEFOS Consortium and the Early Growth Genetics Consortium for their publicly available GWAS summary statistics. We thank Professor Xiao-Chun Bai who generously donated two male *fat-1* TG mice.

Conflict of interest The authors declare that they have no conflict of interest.

Contributors Hong-Wen Deng and Jie Shen conceived and initiated this study together, they provided advice on experimental design and contributed critical suggestions for revision and finalization of the manuscript. Yu-Qian Song performed data and immunohistochemical analyses and drafted the manuscript. Shi-Di Hu, Yin-Hua Zhang Xiao-Wang, Tong Zhang, Chen-Zhong Li, Dao-Yan Pan and Jia-Yi Yang contributed suggestions for immunohistochemical analyses part. Xu Lin, Xiang-He Meng, Cheng Peng, Tao Xu, Rui Gong and Jonathan Greenbaum contributed suggestions for data analyses part. Dong-Yuan Jiang provided me with software technical guidance. Hong-Wen Deng revised and finalized the manuscript. All authors have given critical suggestions for the final version of the manuscript.

References

1. Lin X, Xiong D, Peng YQ, Sheng ZF, Wu XY, Wu XP, Wu F, Yuan LQ, Liao EY (2015) Epidemiology and management of osteoporosis in the People's Republic of China: current perspectives. *Clin Interv Aging* 10:1017–1033. DOI 10.2147/cia.S54613
2. Wright NC, Looker AC, Saag KG, Curtis JR, Delzell ES, Randall S, Dawson-Hughes B (2014) The recent prevalence of osteoporosis and low bone mass in the United States based on bone mineral density at the femoral neck or lumbar spine. *Journal of bone mineral research: the official journal of the American Society for Bone Mineral Research* 29:2520–2526. DOI 10.1002/jbmr.2269
3. Rachner TD, Khosla S, Hofbauer LC (2011) Osteoporosis: now and the future. *Lancet* 377:1276–1287. DOI 10.1016/s0140-6736(10)62349-5
4. Burge R, Dawson-Hughes B, Solomon DH, Wong JB, King A, Tosteson A (2007) Incidence and economic burden of osteoporosis-related fractures in the United States, 2005–2025. *Journal of bone mineral research: the official journal of the American Society for Bone Mineral Research* 22:465–475. DOI 10.1359/jbmr.061113
5. Antoniadou L, MacGregor AJ, Andrew T, Spector TD (2003) Association of birth weight with osteoporosis and osteoarthritis in adult twins. *Rheumatology* 42:791–796. DOI 10.1093/rheumatology/keg227
6. de Bono S, Schoenmakers I, Ceesay M, Mendy M, Laskey MA, Cole TJ, Prentice A (2010) Birth weight predicts bone size in young adulthood at cortical sites in men and trabecular sites in women from The Gambia. *Bone* 46:1316–1321. DOI 10.1016/j.bone.2010.01.381
7. Cooper C, Walker-Bone K, Arden N, Dennison E (2000) Novel insights into the pathogenesis of osteoporosis: the role of intrauterine programming. *Rheumatology* 39:1312–1315. DOI 10.1093/rheumatology/39.12.1312
8. Javaid MK, Arden N, Cooper C (2004) Association of birth weight with osteoporosis and osteoarthritis in adult twins. *Rheumatology* 43:401. DOI 10.1093/rheumatology/keh053
9. Brescianini S, Giampietro S, Cotichini R, Lucchini R, De Curtis M (2012) Genetic and environmental components of neonatal weight gain in preterm infants. *Pediatrics* 129:e455–e459. DOI 10.1542/peds.2010 – 0510
10. Peng C, Shen J, Lin X, Su KJ, Greenbaum J, Zhu W, Lou HL, Liu F, Zeng CP, Deng WF et al (2017) Genetic sharing with coronary artery disease identifies potential novel loci for bone mineral density. *Bone* 103:70–77. DOI 10.1016/j.bone.2017.06.016
11. Kemp JP, Morris JA, Medina-Gomez C, Forgetta V, Warrington NM, Youlten SE, Zheng J, Gregson CL, Grundberg E, Trajanoska K et al (2017) Identification of 153 new loci associated with heel bone mineral density and functional involvement of GPC6 in osteoporosis. *Nat Genet* 49:1468–1475. DOI 10.1038/ng.3949
12. Horikoshi M, Beaumont RN, Day FR, Warrington NM, Kooijman MN, Fernandez-Tajes J, Feenstra B, van Zuydam NR, Gaulton KJ, Grarup N et al (2016) Genome-wide associations for birth weight and

- correlations with adult disease. *Nature* 538:248–252. DOI 10.1038/nature19806
13. Andreassen OA, Thompson WK, Schork AJ, Ripke S, Mattingsdal M, Kelsoe JR, Kendler KS, O'Donovan MC, Rujescu D, Werge T et al (2013) Improved detection of common variants associated with schizophrenia and bipolar disorder using pleiotropy-informed conditional false discovery rate. *PLoS genetics* 9: e1003455. DOI 10.1371/journal.pgen.1003455
 14. Lv WQ, Zhang X, Zhang Q, He JY, Liu HM, Xia X, Fan K, Zhao Q, Shi XZ, Zhang WD et al (2017) Novel common variants associated with body mass index and coronary artery disease detected using a pleiotropic cFDR method. *J Mol Cell Cardiol* 112:1–7. DOI 10.1016/j.yjmcc.2017.08.011
 15. Greenbaum J, Wu K, Zhang L, Shen H, Zhang J, Deng HW (2017) Increased detection of genetic loci associated with risk predictors of osteoporotic fracture using a pleiotropic cFDR method. *Bone* 99:62–68. DOI 10.1016/j.bone.2017.03.052
 16. Videman T, Levalahti E, Battie MC, Simonen R, Vanninen E, Kaprio J (2007) Heritability of BMD of femoral neck and lumbar spine: a multivariate twin study of Finnish men. *Journal of bone mineral research: the official journal of the American Society for Bone Mineral Research* 22:1455–1462. DOI 10.1359/jbmr.070606
 17. Zheng HF, Forgetta V, Hsu YH, Estrada K, Rosello-Diez A, Leo PJ, Dahia CL, Park-Min KH, Tobias JH, Kooperberg C et al (2015) Whole-genome sequencing identifies EN1 as a determinant of bone density and fracture. *Nature* 526:112–117. DOI 10.1038/nature14878
 18. Kichaev G, Roytman M, Johnson R, Eskin E, Lindström S, Kraft P, Pasaniuc B (2017) Improved methods for multi-trait fine mapping of pleiotropic risk loci. *Bioinformatics* 33:248–255. DOI 10.1093/bioinformatics/btw615
 19. Zhang Q, Greenbaum J, Zhang WD, Sun CQ, Deng HW (2018) Age at menarche and osteoporosis: A Mendelian randomization study. *Bone* 117:91–97. DOI 10.1016/j.bone.2018.09.015
 20. Pei YF, Hu WZ, Yan MW, Li CW, Liu L, Yang XL, Hai R, Wang XY, Shen H, Tian Q et al (2018) Joint study of two genome-wide association meta-analyses identified 20p12.1 and 20q13.33 for bone mineral density. *Bone* 110:378–385. DOI 10.1016/j.bone.2018.02.027
 21. Liu YJ, Zhang L, Papasian CJ, Deng HW (2014) Genome-wide Association Studies for Osteoporosis: A 2013 Update. *Journal of bone metabolism* 21:99–116. DOI 10.11005/jbm.2014.21.2.99
 22. Medina-Gomez C, Kemp JP, Dimou NL, Kreiner E, Chesi A, Zemel BS, Bonnelykke K, Boer CG, Ahluwalia TS, Bisgaard H et al (2017) Bivariate genome-wide association meta-analysis of pediatric musculoskeletal traits reveals pleiotropic effects at the SREBF1/TOM1L2 locus. *Nature communications* 8:121. DOI 10.1038/s41467-017-00108-3
 23. Hu Y, Tan LJ, Chen XD, Liu Z, Min SS, Zeng Q, Shen H, Deng HW (2018) Identification of Novel Potentially Pleiotropic Variants Associated With Osteoporosis and Obesity Using the cFDR Method. *J Clin Endocrinol Metab* 103:125–138. DOI 10.1210/jc.2017 – 01531
 24. Maasalu K, Laius O, Zhytnik L, Koks S, Prans E, Reimann E, Martson A (2017) Featured Article: Transcriptional landscape analysis identifies differently expressed genes involved in follicle-

- stimulating hormone induced postmenopausal osteoporosis. *Experimental biology and medicine*. (Maywood NJ) 242:203–213. DOI 10.1177/1535370216679899
25. Mullin BH, Walsh JP, Zheng HF, Brown SJ, Surdulescu GL, Curtis C, Breen G, Dudbridge F, Richards JB, Spector TD et al (2016) Genome-wide association study using family-based cohorts identifies the WLS and CCDC170/ESR1 loci as associated with bone mineral density. *BMC Genomics* 17:136. DOI 10.1186/s12864-016-2481-0
 26. Kemp JP, Medina-Gomez C, Estrada K, St Pourcain B, Heppe DH, Warrington NM, Oei L, Ring SM, Kruithof CJ, Timpson NJ et al (2014) Phenotypic dissection of bone mineral density reveals skeletal site specificity and facilitates the identification of novel loci in the genetic regulation of bone mass attainment. *PLoS Genet* 10:e1004423. DOI 10.1371/journal.pgen.1004423
 27. Workalemahu T, Badon SE, Dishi-Galitzky M, Qiu C, Williams MA, Sorensen T, Enquobahrie DA (2017) Placental genetic variations in vitamin D metabolism and birthweight. *Placenta* 50:78–83. DOI 10.1016/j.placenta.2016.12.028
 28. Fallucca S, Vasta M, Sciuillo E, Balducci S, Fallucca F (2009) Birth weight: genetic and intrauterine environment in normal pregnancy. *Diabetes Care* 32:e149. DOI 10.2337/dc09-1489
 29. Souren NY, Paulussen AD, Steyls A, Loos RJ, Stassen AP, Gielen M, Smeets HJ, Beunen G, Fagard R, Derom C et al (2008) Common SNPs in LEP and LEPR associated with birth weight and type 2 diabetes-related metabolic risk factors in twins. *International journal of obesity (2005)* 32: 1233–1239. DOI 10.1038/ijo.2008.68
 30. Charalambous M, Smith FM, Bennett WR, Crew TE, Mackenzie F, Ward A (2003) Disruption of the imprinted Grb10 gene leads to disproportionate overgrowth by an Igf2-independent mechanism. *Proc Natl Acad Sci USA* 100:8292–8297. DOI 10.1073/pnas.1532175100
 31. Hill DJ, Petrik J, Arany E (1998) Growth factors and the regulation of fetal growth. *Diabetes Care* 21(Suppl 2):B60–B69
 32. Schroeder JW, Conneely KN, Cubells JC, Kilaru V, Newport DJ, Knight BT, Stowe ZN, Brennan PA, Krushkal J, Tylavsky FA et al (2011) Neonatal DNA methylation patterns associate with gestational age. *Epigenetics* 6:1498–1504. DOI 10.4161/epi.6.12.18296
 33. Alexandre-Gouabau MC, Bailly E, Moyon TL, Grit IC, Coupe B, Le Drean G, Rogniaux HJ, Parnet P (2012) Postnatal growth velocity modulates alterations of proteins involved in metabolism and neuronal plasticity in neonatal hypothalamus in rats born with intrauterine growth restriction. *J Nutr Biochem* 23:140–152. DOI 10.1016/j.jnutbio.2010.11.008
 34. Laviola L, Perrini S, Belsanti G, Natalicchio A, Montrone C, Leonardini A, Vimercati A, Scioscia M, Selvaggi L, Giorgino R et al (2005) Intrauterine growth restriction in humans is associated with abnormalities in placental insulin-like growth factor signaling. *Endocrinology* 146:1498–1505. DOI 10.1210/en.2004 – 1332
 35. Chun SK, Shin S, Kim MY, Joung H, Chung J (2017) Effects of maternal genetic polymorphisms in vitamin D-binding protein and serum 25-hydroxyvitamin D concentration on infant birth weight. *Nutrition (Burbank Los Angeles County Calif)* 35:36–42. DOI 10.1016/j.nut.2016.10.006

36. Teng RJ, Wu TJ, Hsieh FJ (2015) Cord blood level of insulin-like growth factor-1 and IGF binding protein-3 in monozygotic twins. *Journal of the Formosan Medical Association = Taiwan yi zhi* 114:359–362. DOI 10.1016/j.jfma.2012.12.014
37. Joung KE, Cataltepe SU, Michael Z, Christou H, Mantzoros CS (2017) Cord Blood Adipocyte Fatty Acid-Binding Protein Levels Correlate With Gestational Age and Birth Weight in Neonates. *J Clin Endocrinol Metab* 102:1606–1613. DOI 10.1210/jc.2016–3831
38. Lemaitre RN, Tanaka T, Tang W, Manichaikul A, Foy M, Kabagambe EK, Nettleton JA, King IB, Weng LC, Bhattacharya S et al (2011) Genetic loci associated with plasma phospholipid n-3 fatty acids: a meta-analysis of genome-wide association studies from the CHARGE Consortium. *PLoS genetics* 7: e1002193. DOI 10.1371/journal.pgen.1002193
39. Guan W, Steffen BT, Lemaitre RN, Wu JHY, Tanaka T, Manichaikul A, Foy M, Rich SS, Wang L, Nettleton JA et al (2014) Genome-wide association study of plasma N6 polyunsaturated fatty acids within the cohorts for heart and aging research in genomic epidemiology consortium. *Circulation Cardiovascular genetics* 7:321–331. DOI 10.1161/circgenetics.113.000208
40. Cinelli G, Fabrizi M, Rava L, Signore F, Vernocchi P, Semeraro M, Vallone C, Lanciotti R, Ciofi Degli Atti M, Manco M (2018) Association between Maternal and Foetal Erythrocyte Fatty Acid Profiles and Birth Weight. *Nutrients* 10. DOI 10.3390/nu10040402
41. Longo AB, Ward WE (2016) PUFAs, Bone Mineral Density, and Fragility Fracture: Findings from Human Studies. *Advances in nutrition. (Bethesda Md)* 7:299–312. DOI 10.3945/an.115.009472
42. Orchard TS, Ing SW, Lu B, Belury MA, Johnson K, Wactawski-Wende J, Jackson RD (2013) The association of red blood cell n-3 and n-6 fatty acids with bone mineral density and hip fracture risk in the women's health initiative. *Journal of bone mineral research: the official journal of the American Society for Bone Mineral Research* 28:505–515. DOI 10.1002/jbmr.1772
43. Huang MJ, Wang L, Jin DD, Zhang ZM, Chen TY, Jia CH, Wang Y, Zhen XC, Huang B, Yan B et al (2014) Enhancement of the synthesis of n-3 PUFAs in fat-1 transgenic mice inhibits mTORC1 signalling and delays surgically induced osteoarthritis in comparison with wild-type mice. *Ann Rheum Dis* 73:1719–1727. DOI 10.1136/annrheumdis-2013-203231
44. Horikoshi M, Yaghoobkar H, Mook-Kanamori DO, Sovio U, Taal HR, Hennig BJ, Bradfield JP, St Pourcain B, Evans DM, Charoen P et al (2013) New loci associated with birth weight identify genetic links between intrauterine growth and adult height and metabolism. *Nat Genet* 45:76–82. DOI 10.1038/ng.2477
45. Kuipers A, Zhang Y, Cauley JA, Nestlerode CS, Chu Y, Bunker CH, Patrick AL, Wheeler VW, Hoffman AR, Orwoll ES et al (2009) Association of a high mobility group gene (HMGA2) variant with bone mineral density. *Bone* 45:295–300. DOI 10.1016/j.bone.2009.04.197
46. Rivadeneira F, Houwing-Duistermaat JJ, Vaessen N, Vergeer-Drop JM, Hofman A, Pols HA, Van Duijn CM, Uitterlinden AG (2003) Association between an insulin-like growth factor I gene promoter polymorphism and bone mineral density in the elderly: the Rotterdam Study. *J Clin Endocrinol Metab* 88:3878–3884. DOI 10.1210/jc.2002–021813

47. Gutierrez GM, Kong E, Sabbagh Y, Brown NE, Lee JS, Demay MB, Thomas DM, Hinds PW (2008) Impaired bone development and increased mesenchymal progenitor cells in calvaria of RB1^{-/-} mice. *Proc Natl Acad Sci USA* 105:18402–18407. DOI 10.1073/pnas.0805925105
48. Wu C, Orozco C, Boyer J, Leglise M, Goodale J, Batalov S, Hodge CL, Haase J, Janes J, Huss JW 3rd, et al (2009) BioGPS: an extensible and customizable portal for querying and organizing gene annotation resources. *Genome biology* 10:R130. DOI 10.1186/gb-2009-10-11-r130
49. Weiss LA, Barrett-Connor E, von Muhlen D (2005) Ratio of n-6 to n-3 fatty acids and bone mineral density in older adults: the Rancho Bernardo Study. *Am J Clin Nutr* 81:934–938. DOI 10.1093/ajcn/81.4.934
50. Calder PC (2011) Fatty acids and inflammation: the cutting edge between food and pharma. *European journal of pharmacology* 668 Suppl 1: S50-58. DOI 10.1016/j.ejphar.2011.05.085

Figures

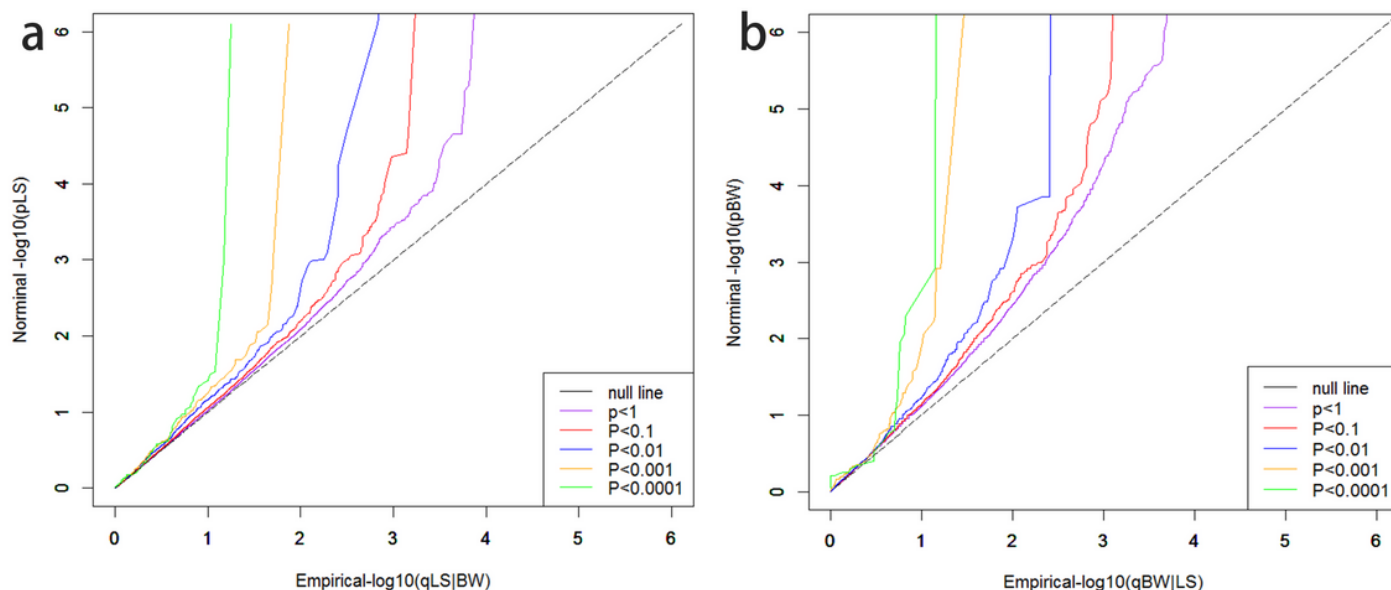


Figure 1

Q-Q plots Stratified Q-Q plots of nominal versus empirical $-\log_{10}$ p-values for (a) LS BMD as a function of significance of the association with BW, and (b) BW as a function of significance of the association with LS BMD. The level of $-\log_{10}(p) > 0$, $-\log_{10}(p) > 1$, $-\log_{10}(p) > 2$, $-\log_{10}(p) > 3$ correspond to $p < 1$, $p < 0.1$, $p < 0.01$, $p < 0.001$ respectively.

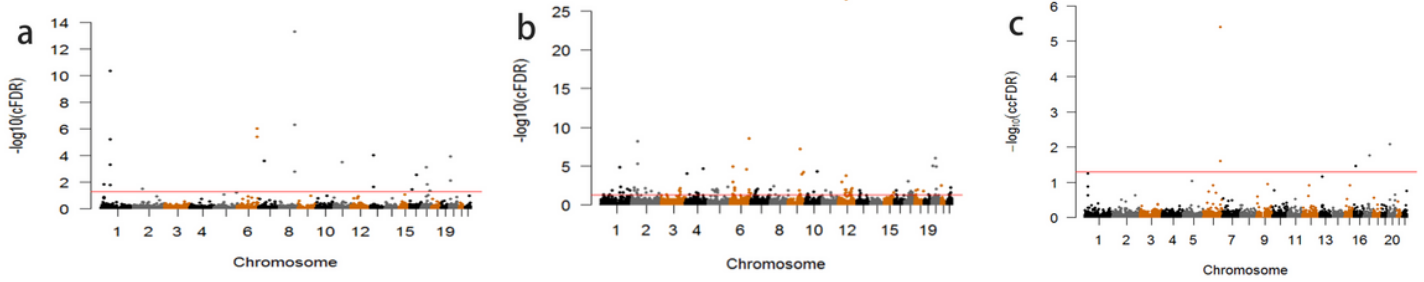


Figure 2

Manhattan plots a) Conditional Manhattan plot of conditional $-\log_{10}$ FDR values for LS BMD given BW (LS BMD|BW); b) Conditional Manhattan plot of conditional $-\log_{10}$ FDR values for BW given LS BMD (BW|LS BMD); c) Conjunction Manhattan plot of conjunction $-\log_{10}$ FDR values for LS BMD and BW. The red line corresponds to conditional $-\log_{10}$ FDR value of 1.3 (cFDR < 0.05).

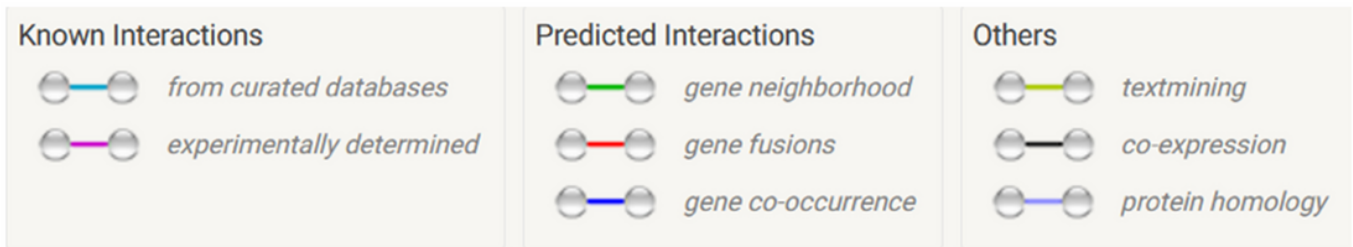
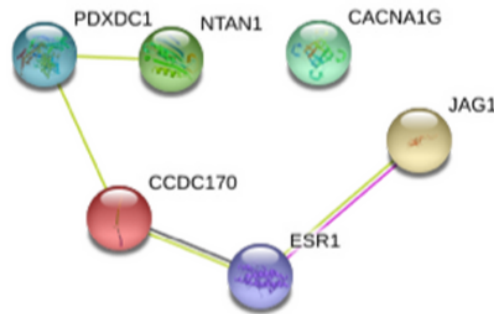


Figure 3

Protein-protein interaction network Protein-protein interaction network for cFDR-significant pleiotropic susceptibility genes. Connections were based on evidence with an interaction score ≥ 0.40 . Network nodes represent proteins produced by the corresponding genes, edges between nodes indicate protein-protein associations, edge color indicates the type of interaction and is specified on the bottom of the figure.

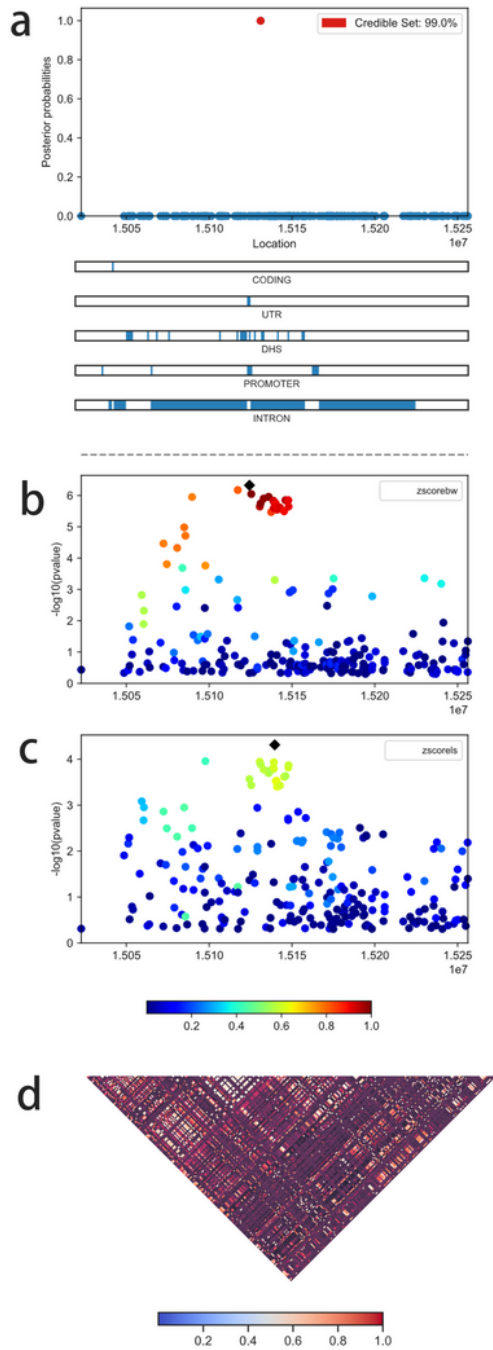


Figure 4

Visualization of Posterior Probability Plots We present (a) posterior probability of each SNP, (b) Z-score for BW, (c) Z-score for LS BMD, and (d) LD matrix.

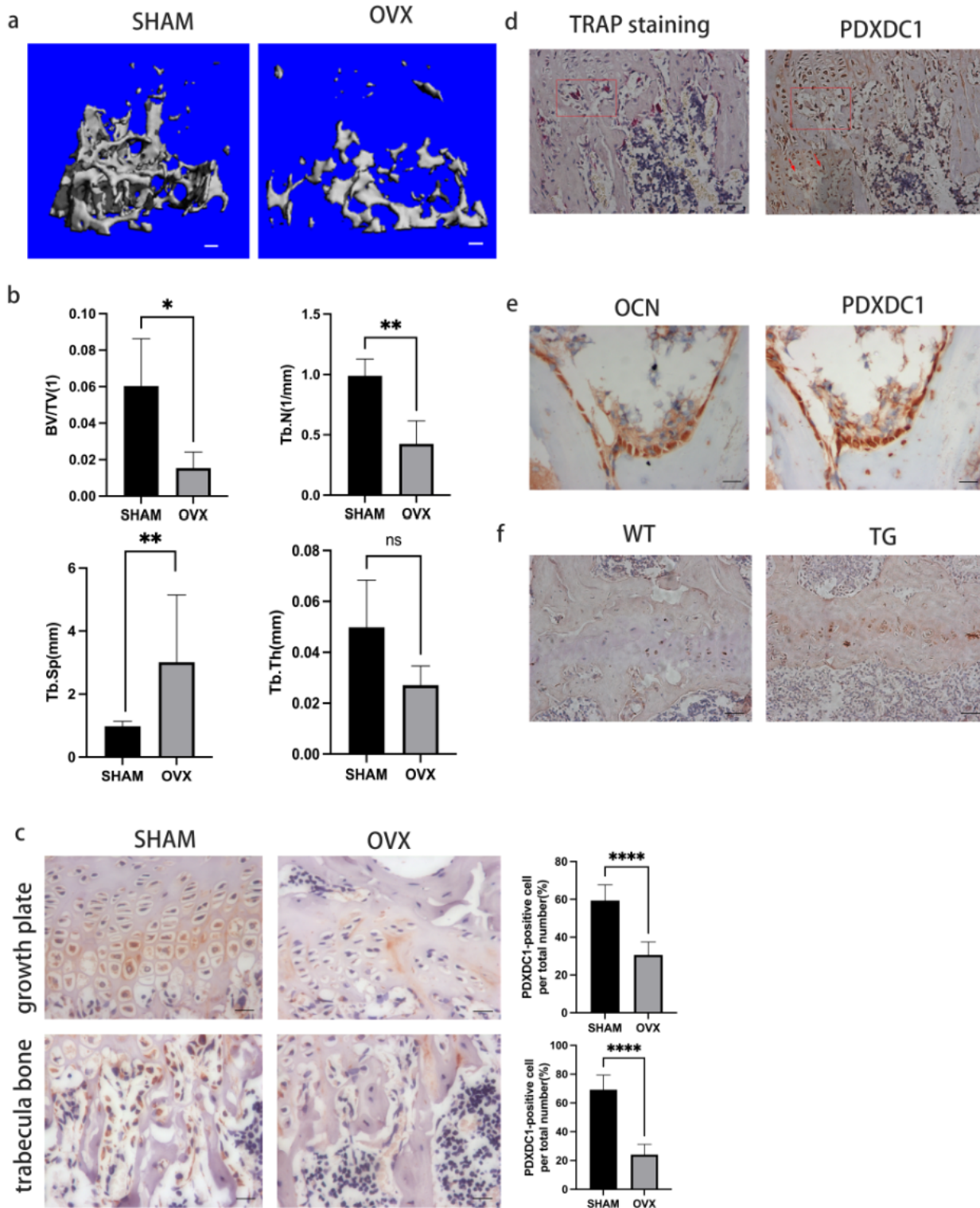


Figure 5

Partially validation of PDXDC1 (a) Micro-computed tomography scanner assessment of trabecular bone microstructural parameters. Three-dimensional microstructural of trabecular bone of SHAM group and OVX group by micro-CT scanner at 16 weeks after operation. Scale bar, 100 μ m. (b) Morphological analysis between SHAM group and OVX group of BV/TV, Tb. Th, Tb. N and Tb. Sp. n=4 per group. Data represent mean \pm SD. * $p < 0.05$, ** $p < 0.01$. (c) Immunostaining and quantification analysis of PDXDC1

between SHAM group and OVX group at growth plate and trabecula bone. Higher expression of PDXDC1 is related to higher BMD. Scale bar, 20 μm . $n=4$ per group. Data represent mean \pm SD. **** $p < 0.0001$. (d, e) Immunohistochemistry assay with serial sections of SHAM group. Both osteoclasts and osteoblasts express PDXDC1. Scale bar of d, 50 μm . Scale bar of e, 20 μm . (f) Immunostaining of PDXDC1 of transgenic (TG) mice and wild-type (WT) mice. Higher expression of PDXDC1 is related to lower ratio n-6/n-3 PUFA. Scale bar, 50 μm .

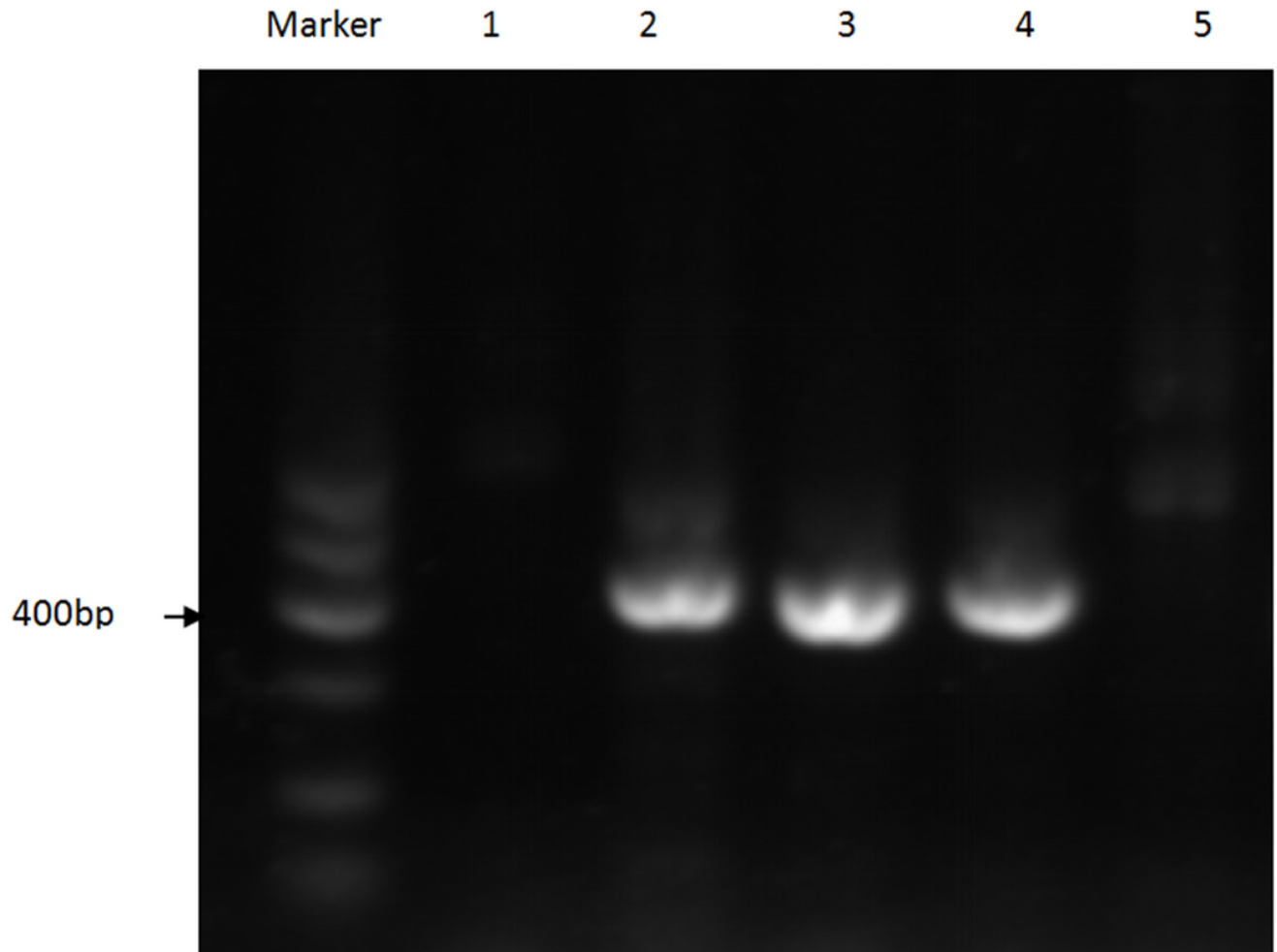


Figure 6

fat-1 TG mice identification PCR genotyping identification with fat-1 fragment-specific primers. Line 2, 3 and 4 indicated fat-1 gene expression; line 1 and 5 indicated wild-type (WT) gene expression.

Supplementary Files

This is a list of supplementary files associated with this preprint. Click to download.

- [OnlineResource1.pdf](#)
- [OnlineResource2.pdf](#)

- [OnlineResource3.pdf](#)